MONTE CARLO DOSE CALCULATION OF *RHIZOPHORA SPP.* SOY PROTEIN PHANTOM AT RADIOTHERAPY ENERGY RANGE

NOR AIN BINTI RABAIEE

UNIVERSITI SAINS MALAYSIA

2018

MONTE CARLO DOSE CALCULATION OF *RHIZOPHORA SPP.* SOY PROTEIN PHANTOM AT RADIOTHERAPY ENERGY RANGE

by

NOR AIN BINTI RABAIEE

Thesis submitted in fulfilment of the requirements

for the degree of

Doctor of Philosophy

February 2018

ACKNOWLEDGEMENT

"In the name of Allah, the Most Gracious, the Most Merciful"

All the praises be to Allah, the Lord of the worlds, peace and blessing be upon the Prophet Muhammad S.A.W. Highest gratitude to Allah, who gives the knowledge to whom He wills, inspires when deadlock, which paves the way when in troubles, gives the strength when feel week. With the help and permission from Him, this thesis could be finished.

My highest appreciation goes to my supervisor, Dr Mohd Zahri bin Abdul Aziz, who are truly guide me all the way of this journey. Thanks for the wonderful opportunity. I would like to thanks my co-supervisor, Prof Rokiah Hashim, the one who always motivate me towards the end of my journey, even with her tight schedule. The appreciation also extended to Prof Abdul Aziz Tajuddin and Dr Ahmad Lutfi. May Allah reward them with the kindness.

I also want to acknowledge the Ministry of Higher Education for the MyPHD scholarship (KPM(B) 891214135886) and the fundamental Research Grant Scheme (FRGS) 203/CIPPT/6711341 for providing a fund during period of this study.

The appreciation also goes to everyone who helped me throughout my study, especially Mr Reduan and Ms Shazleen from USM Kubang Kerian, Mr. Basrol from School of Industrial Technology, Mr Rizal and Mr Hazhar from School of Physics and all staffs at the Department of Oncological and Radiological Science, AMDI. Thanks to my fellow friends from Medical Physics team. May Allah grants success to all of you.

I also would like to take this opportunity to express my deepest appreciation to my parents, Haji Rabaiee Omar and Hajah Rukiah Abdul Aziz, thanks for the endless support, prayers and well raising me and siblings. May Allah forgives and blesses them. My special appreciation goes to my love of my life, Muhammad Fadhirul Izwan Abdul Malik, who loyally together with me, up and down, cries and laugh. The person who are mutually compromise and willing to share feelings, views, even criticism when needed. Thank you for the priceless sacrifices and to our greatest gift, Muhammad Zaheen Muttaqin. I dedicated this thesis to you, to inspire you in the future. May you be faithful person, good character and useful for the society.

Last but not least, hopefully this small writing will bring beneficial knowledge and every effort that has been contributed is rewarded by Allah.

Alhamdulillah, this is for you, Ayah, Mak.

TABLE OF CONTENT

CHAPTER 1

INTRODUCTION

CHAPTER 2

THEORY AND LITERATURE REVIEW

CHAPTER 3

FABRICATION AND CHARACTERISATION OF *RHIZOPHORA SPP.* SOY PROTEIN PARTICLEBOARD

CHAPTER 4

CONSTRUCTION AND BENCHMARKING OF THE LINAC TREATMENT HEAD MC MODELS FOR PHOTON AND ELECTRON BEAM

CHAPTER 5

DOSE DISTRIBUTION IN *RHIZOPHORA SPP.* SOY PROTEIN PHANTOM

CHAPTER 6

CONCLUSION AND RECOMMENDATIONS

APPENDICES

LIST OF PUBLICATIONS

LIST OF FIGURES

LIST OF TABLES

LIST OF ABBREVIATIONS AND SYMBOLS

1-D	One dimensional
2-D	Two dimensional
3-D	Three-dimensional
%	Percentage
˚C	Degree in Celcius
µm	micrometer
AAPM	American Association of Physicist in Medicine
AE	Electron production cut-off energy
Ag	Argentum
AP	Photon production cut-off energy
BEAMdp	Beam data processor
cGy	centiGray
CHNS/O	Carbon, hydrogen, nitrogen, sulfur/oxygen
cm	centimeter
Co-60	Cobalt-60
CT	Computed tomography
DBS	Directional Bremsstrahlung Splitting
DICOM	Digital imaging and communication in medicine
Dmax	Dose at maximum depth
dmax	Depth at maximum dose
d80	Depth at 80 % of maximum dose
d90	Depth at 90 % of maximum dose
d50	Depth at 50 % of maximum dose

e/cm^3	Number of electron per centimeter cubic
EBT	Extended Beam Therapy
ECUT	Electron cut-off
EGSnrc	Electron Gamma Shower by National Research Council
FESEM	Field emission scanning electron microscopy
g	Gram
g/cm^3	Gram per centimeter cubic
GEANT	Geometry and Tracking
FWHM	Full width half maximum
h	Hour
HU	Hounsfield Unit
HUSM	Hospital Universiti Sains Malaysia
IB	Internal Bonding
IC	Ionisation Chamber
ICRU	International Commissioning of Radiation Units and Measurement
JIS	Japanese International Standard
keV	Kilo electron volt
kg	Kilogram
LEGe	Low Energy Germanium
LINAC	Linear Accelerator
m	Meter
MC	Monte Carlo
MCNP	Monte Carlo Neutron Positron
MeV	Mega electron volt
min	Minute

MLC	Multileaf Collimator
mm	Milimeter
mm/min	Milimeter per minute
Mo	Molybdenum
MPa	Mega Pascal
MU	Monitor Unit
MU/cGy	Monitor unit per centiGray
MV	Megavoltage
N/mm^2	Newton per milimeter square
NIST	National of Institute Standard Technology
OAR	Organ at risk
PAE	Polyamidoamine-epichlorohydrin
PCUT	Photon cut-off energy
PDD	Percentage depth dose
PEEC	Phantom embedded extrapolation chamber
PEGS4	Pre-electron gamma shower
PENELOPE	Energy loss of positron and electron
PF	Phenol formaldehyde
PMMA	Polymethylethacrylate
PRF	Phenol resorcinol formaldehyde
QA	Quality Assurance
ROI	Region of interest
Rp	Practical range
SBS	Selective bremsstrahlung splitting
Sn	Tin

SPSS	Statistical programme for social science
SSD	Source to surface distance
TIFF	Tagged image file format
TLD	Thermoluminescent detector
TPS	Treatment planning system
TS	Thickness swelling
UBS	Uniform bremsstrahlung splitting
UF	Urea formaldehyde
UTM	Universal tensile machine
VRT	Variance rejection technique
WA	Water absorption
XCOM	X-ray computed
XRF	X-ray fluorescence
Z	Atomic number
Z_{eff}	Effective atomic number
Zr	Zirconium

PENGIRAAN DOS MONTE CARLO DALAM FANTOM *RHIZOPHORA SPP.* PROTIN SOYA PADA JULAT TENAGA RADIOTERAPI

ABSTRAK

Pokok kayu bakau Malaysia, *Rhizophora spp.* telah di kaji secara meluas untuk potensinya sebagai sifat setara tisu. Walau bagaimanapun, kayu *Rhizophora spp.* yang tidak di rawat tidak sesuai untuk dijadikan fantom disebabkan oleh sifat fizikalnya. Oleh itu, papan partikel *Rhizophora spp.* yang dirawat telah dicadangkan sebagai alternatif. Kajian ini bertujuan untuk meneroka potensi papan partikel *Rhizophora spp.* yang dirawat sebagai bahan fantom dengan menggunakan kaedah Monte Carlo pada julat tenaga radioterapi. Kajian ini dimulakan dengan memilih campuran terbaik bagi *Rhizophora spp.* dengan protin soya berdasarkan ciri pengelasan seperti ketumpatan, ketumpatan elektron, kestabilan dimensi, pekali pengecil dan nombor atom efektif. Penambahan protin soya sebagai bahan perikat menghasilkan peningkatan yang siknifikan kepada kestabilan dimensi papan partikel. *Rhizophora spp.* dengan saiz partikel 50 – 104 µm dan 8 % protin soya di pilih sebagai campuran terbaik. Campuran tersebut kemudiannya digunakan bagi mengolah fantom dengan pelbagai ketebalan (0.4 cm, 0.5 cm, 0.6 cm, 0.7 cm, 0.8 cm and 0.9 cm) dan ketumpatan (di antara 0.99 dan 1.06 g/cm^3). Dalam masa yang sama, model pecutan lurus (LINAC) Primus untuk sinar foton (6 dan 10 MV) dan elektron (6 dan 15 MeV) dihasilkan menggunakan kod EGSnrc/BEAMnrc, manakala taburan dos dikira menggunakan kod EGSnrc/DOSXYZnrc. Fantom pepejal air yang komersial digunakan sebagai rujukan, untuk mensahihkan keputusan fantom *Rhizophora spp.* protin soya. Keputusan peratusan kedalaman dos (PDD) untuk tenaga foton pada kedalaman dos maksimum, dmax bagi fantom *Rhizophora spp.*

protin soya adalah selari dengan fantom air. Sementara itu, bagi sinar tenaga elektron, keputusan yang setara di antara fantom telah di kenal pasti. Taburan dos dalam kedua-dua fantom juga di ukur menggunakan filem Gafkromik EBT2. Keputusan yang setara direkodkan di antara fantom, dengan perbezaan peratusan di antara 10 dan 3 % pada keseluruhan kedalaman, untuk sinar tenaga foton 6 dan 10 MV. Taburan dos untuk 6 dan 15 MeV yang juga diukur menggunakan filem EBT2 dijumpai bersesuaian dengan fantom pepejal air, dengan perbezaan di antara 6 dan 4 %, masing-masingnya, pada setiap kedalaman. Profil sinaran untuk kesemua tenaga sinar foton dan elektron bagi fantom *Rhizophora spp.* protin soya menunjukkan kelurusan yang baik, selari dengan fantom pepejal air. Dalam kajian ini, potensi fantom *Rhizophora spp.* protin soya sebagai bahan setara air telah berjaya diterokai, sementara model Primus LINAC telah berjaya dihasilkan menggunakan kod EGSnrc. Secara keseluruhannya, keputusan daripada hasil kajian ini telah berjaya memenuhi kesemua objektif kajian.

MONTE CARLO DOSE CALCULATION OF *RHIZOPHORA SPP.* SOY PROTEIN PHANTOM AT RADIOTHERAPY ENERGY RANGE

ABSTRACT

The Malaysian mangrove hardwood, *Rhizophora spp.* has been extensively studied as a potential tissue equivalent material. However, the untreated *Rhizophora spp.* wood is unsuitable to be used as a phantom, due to its physical properties. Thus, the treated *Rhizophora spp.* particleboard was suggested as an alternative. The aim of this study was to explore the *Rhizophora spp.* particleboard with soy protein adhesive, as a potential phantom material, with its application validated using the Monte Carlo (MC) method at the radiotherapy energy range. The work was initiated by choosing the best mixture of the *Rhizophora spp.* with soy protein, based on its characteristics, i.e. density, electron density, dimensional stability, attenuation coefficient and effective atomic number. The addition of soy protein as an adhesive has resulted in a significant improvement in the particleboard's dimensional stability. The *Rhizophora spp.* with particle size of 50–104 µm and 8 % soy protein has been chosen as the best mixture. The mixture was then used to fabricate the phantom with various thicknesses (0.4, 0.5, 0.6, 0.7, 0.8 and 0.9 cm) and densities (between 0.99 and 1.06 g/cm^3). Meanwhile, the PRIMUS linear accelerator (LINAC) with photon (6 and 10 MV) and electron (6 and 15 MeV) beams were modelled using the EGSnrc/BEAMnrc code, while the dose distributions were calculated using the EGSnrc/DOSXYZnrc code. A commercial solid water phantom was used as a reference, to validate the performance of the *Rhizophora spp.* soy protein phantom. The percentage depth dose (PDD) result for the photon beam energies shows that the depth of maximum dose, dmax for the *Rhizophora spp.* soy protein phantom was identical with that of the standard water phantom. Meanwhile, for electron beam energies, a comparable result between these phantoms was observed. Dose distributions in the phantoms were also measured using Gafchromic EBT2 films. Comparable results were recorded between the phantoms, with percentage differences of within 10 and 3 % at all measured depths, for 6 and 10 MV photon beam energies, respectively. The dose distribution at 6 and 15 MeV measured using the EBT2 films were found to be comparable to that of the solid water phantom, with discrepancies of within 6 and 4 %, respectively, at all measured depths. The beam profiles for all photon and electron beam energies for *Rhizophora spp.* soy protein phantom showed good flatness, and consistent with the solid water phantom. In this study, the potential of the *Rhizophora spp.* soy protein phantom as a water equivalent material has been successfully explored, while a PRIMUS LINAC model has been established using the EGSnrc code. Overall, the results obtained in this study have been successfully fulfilled all the study's objectives.

CHAPTER 1

INTRODUCTION

1.1 Background

The linear accelerator (LINAC) is the most common modality used in the field of radiotherapy. It can generate and deliver high energy range of both photon and electron beams. In most common practice, radiotherapy is combined with either surgery or chemotherapy, etc.

The goal of radiotherapy is to deliver the highest possible dose to the target tumour, while sparing the surrounding healthy tissues. In order to achieve this, the performance of the LINAC should be regularly checked or calibrated prior to clinical use, to ensure that it works optimally by delivering the exact dose as planned in the Treatment Planning System (TPS).

The calibration should be done in terms of the LINAC's output and beam quality, based on the Quality Assurance (QA) programme (Jarkko, 2014). The QA programme consists of two objectives (Khan, 2010), to ensure that the dose is being accurately delivered as prescribed/planned, and to avoid unnecessary exposure to the healthy tissues.

Water phantom is typically used as the gold standard in the QA programme, as it is being considered as the perfect representation of the human soft tissue. However, in the field of radiotherapy, handling a large amount of liquid water is not always practical, since the LINAC is composed of electronic devices that are mostly non-waterproof. Therefore, the solid water phantom has been commonly used as an alternative to the liquid water phantom.

Polystyrene, acrylic and other proprietary materials, are the examples of commercial water equivalent materials that are extensively used as phantoms for radiation dosimetry. However, due to the high costs, some institutions cannot afford to provide these types of solid phantom materials. Thus, some developing countries have started to investigate other options of materials, which can provide similar characteristics as the commercial solid phantoms and made from locally available raw materials with affordable prices (Hossen and Pabna, 2016).

Since the early 90s, an extensive study has been reported on the linear attenuation coefficient of the *Rhizophora spp.* wood. Thus, this has attracted many researchers to explore the potential of these wood, as a water equivalent material (Abuarra et al., 2014; Tousi et al., 2014; Shakhreet et al., 2009).

Treatment planning involving the dose distributions on the target tumour, surrounding tissues and the organ at risk (OAR), are calculated using the algorithm in the TPS. The dose received by the tumour should be the highest, so as to be able to preserve the surrounding healthy tissues and the OARs.

There are various algorithms that are commonly used in the TPS, to calculate the dose distributions, e.g. pencil-beam, pencil-beam redefinition, collapsed cone convolution and superposition/convolution algorithms. Generally, the algorithm works based on the basic physics of radiation interaction in a tissue. Since this physics concept can be very complex, it has been simplified to shorten the calculation time. However, this simplification has resulted in some inherent uncertainties (Khan, 2010).

In contrast, Monte Carlo (MC) is a complex algorithm that has been well known as an advance, accurate and reliable method for dose calculation in radiotherapy. However, a much detail information is compulsory for this algorithm to carry out its calculation, which consequently results in a longer calculation time.

The advantage of the MC method compared to the conventional TPS is the possibility to meet the uncertainties of between 2–3 %. It has also been recommended as a solution for various complex mathematical problems (Reynaert et al., 2007).

The MC method relies on the fundamental of high energy radiations, including the photon and electron beams from the LINAC that were imparted to a patient. MC algorithm integrates mathematical model, as well as advanced computing knowledge into the treatment planning process (Caccia et al., 2007).

Another important factor related to the dosimetric properties in radiotherapy is the treatment machine output. The differences between the doses delivered by the LINAC should be less than 3 % compared to the doses planned in the TPS. Failure to achieve this will result in an underdose to the target tumour, with unnecessary exposure to the healthy tissues.

The high accuracy of the MC method is important to calculate the dose distribution in the phantom. Thus, the probability of interactions between the x-rays and the fabricated phantom were employed in this study. The results obtained from this study is important to increase the marketability of this Malaysian hardwood, i.e. *Rhizophora spp.*, as an alternative water equivalent material for dosimetric purposes. Figure 1.1 illustrate the workflow of this study.

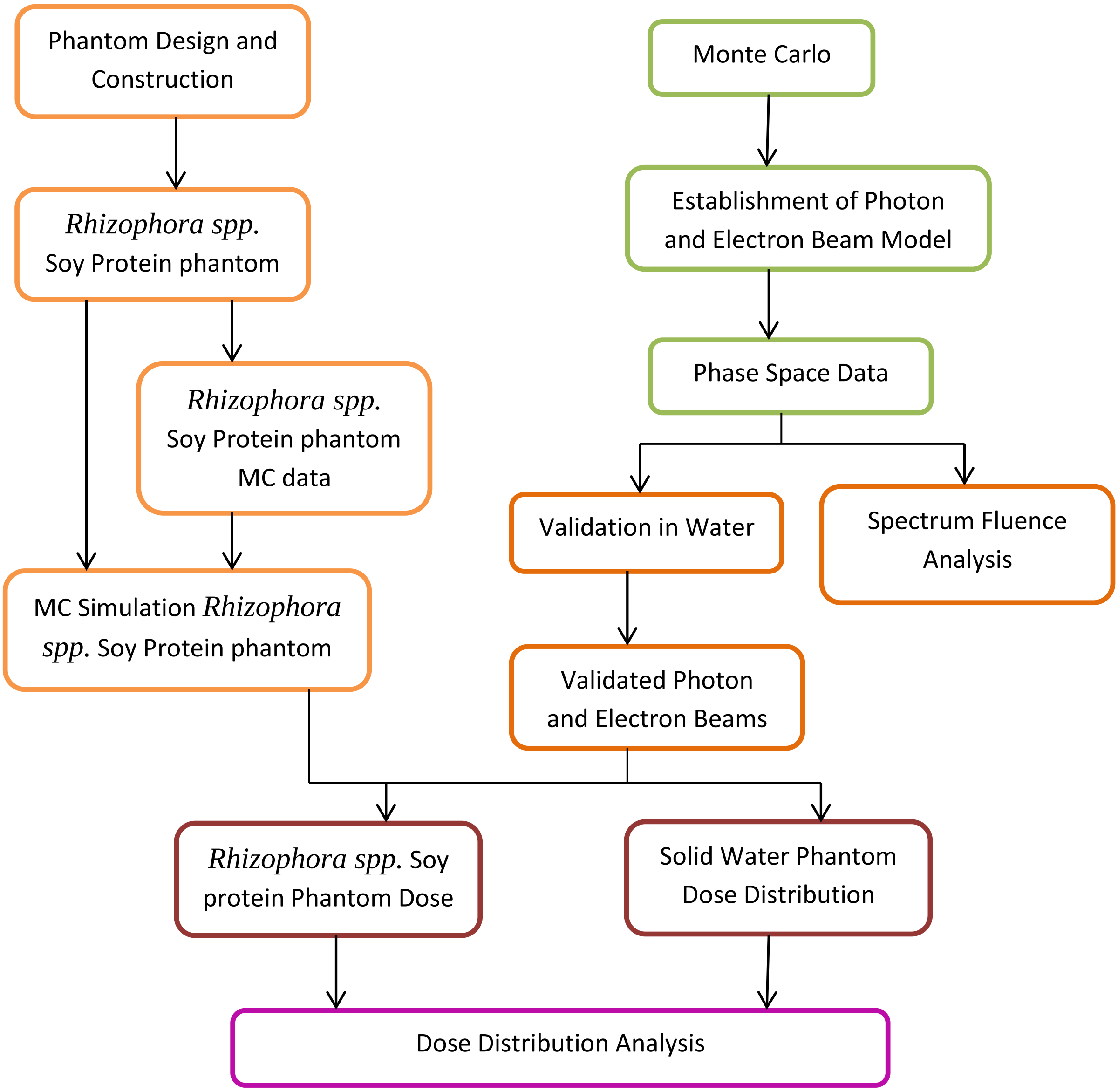

Figure 1.1: The workflow to determine the dose distribution within the phantoms.

1.2 Problem Statement

The current algorithm used in the TPS is limited to the parameters provided by the manufacturer (Khan, 2010). This has resulted in a larger deviation, especially when the tissue inhomogeneity and density variations were taken into account. Therefore, the MC method that has been well known as the most accurate algorithm will be very helpful, to reduce the uncertainties in the dose calculation (Kim, Robin and Zdenka, 2012).

Water has been recommended as the preferred medium in the standard dosimetry protocol for high energy x-ray, as it was found to have the closest attenuation and scattering properties to the human soft tissue. Unfortunately, water in the form of liquid, is time consuming to be positioned and aligned with the radiation beam, which might affect the routine procedure in the department. There are also difficulties in maintaining the temperature and humidity of the water phantom and its surrounding (Hossen & Pabna, 2016). Moreover, some of the dosimeters were not made with the waterproof feature. Thus, the solid water phantom is expected to be more convenient for the use of routine QA in radiotherapy.

Numerous water equivalent materials, such as polystyrene, acrylic and solid water have been developed (Vasiliev et al., 2010; Banjade et al., 2001). However, they have a limitation in mimicking the real human soft tissue (Yohannes et al., 2012; Hill et al., 2008). Besides, some of them were unable to offer comparable dosimetric properties as water, at low and high energy ranges. Furthermore, there is a variation in the elemental composition of these water equivalent materials, and there are also some solid water equivalent materials that were given similar names, but differ in terms of the mixtures and formulations (Yohannes et al., 2012; Nisbet et al., 1999).

The Malaysian mangrove hardwood, *Rhizophora spp.* has been extensively studied by previous researchers and was noted to have the potential as a tissue equivalent material. Many authors have also reported that the attenuation properties of this wood matches with water and the breast tissue (Shakhreet et al., 2013; Marashdeh et al., 2012; Bauk & Tajuddin, 2008). However, the *Rhizophora spp.* wood may not be suitable to be directly used as a phantom, as it is heavy and has the potential to crack and wrap after a long time. Another issue is the limitation of the trunk diameter and the inhomogeneous density of the raw wood, which makes it unsuitable to be use as a phantom. Therefore, the *Rhizophora spp.* was customised into a particleboard that has a homogenous density, with the desired dimension and thickness.

Previous study on the fabrication of the *Rhizophora spp.* particleboard was focused mainly on its application in diagnostic imaging and at low photon energy (Tousi et al., 2017; Ababneh, 2016; Abuarra, 2014). Thus, a potential phantom intended for application at the radiotherapy energy range was fabricated in this study. The fabricated phantom was made from locally available materials, inexpensive and equally excellent in quality, and thus, will be beneficial as an alternative water equivalent phantom.

1.3 Objectives

The aim of this study was to develop a phantom from the *Rhizophora spp.* soy protein particleboard with comparable dosimetric properties as the commercial solid water phantom, for application in radiotherapy. The phantom was then validated using the PRIMUS LINAC model generated using the Monte Carlo method. In order to achieve this aim, the following objectives were fulfilled, which include:

I. To fabricate and characterise the *Rhizophora spp.* particleboard bonded with soy protein,

II. To provide radiation data of the *Rhizophora spp.* soy protein phantom, as input for the MC calculation (i.e. linear attenuation coefficient and probability of interaction data).

III. To establish a validated Monte Carlo photon and electron beam models from the Primus LINAC.

IV. To compare the dosimetric properties of the *Rhizophora spp.* soy protein phantom with a solid water phantom, using the Monte Carlo method.

V. To determine the potential use of the *Rhizophora spp.* soy protein phantom as a water equivalent material via the Monte Carlo validation.

1.4 Significant of Study

This work involved the investigation on the potential of the *Rhizophora spp.* soy protein phantom as a water equivalent material, and the development of the PRIMUS LINAC model using the MC method for dose verification. Radiation simulation at high energy range using the MC method can be useful to extend the marketability of the *Rhizophora spp.* soy protein phantom. In-vivo dose measurements have also been conducted in this study. The *Rhizophora spp.* soy protein phantom for radiotherapy dosimetry is advantageous as it was made from readily available formaldehyde-free local material.

On the other hand, the phase space files of the PRIMUS LINAC generated from this study can be submitted and proposed to the International Atomic Energy Agency (IAEA) database, to be used by other users worldwide. These files can be used to develop a virtual source model, for both photon and electron beams. As of this date, only the phase space files of the PRIMUS LINAC with 6 MV photon beam are available in the IAEA database. Thus, our data can be very helpful for the beginner users of MC, to establish their own virtual source model from the current phase space files.

1.5 Thesis Outline

This thesis consists of six chapters. Chapter one entails the introduction of this study, which include the background of study, problem statement, objectives, significance of study and the thesis outline. Chapter two consists of the literature review, which highlights the theoretical aspects of the MC method, *Rhizophora spp.* wood, soy protein and Gafchromic film dosimeter. The commercial water equivalent phantoms that are commonly used in the radiotherapy dosimetry were also discussed in this chapter. Chapter three covers the fabrication and characterisation of the

Rhizophora spp. soy protein phantom. The preliminary work, the rational of the fabrication approach, as well as the limitations of the fabricated phantom were also discussed in this chapter. Chapter four includes the modelling and dose verification of the PRIMUS LINAC. The application of the fabricated phantom, i.e. the *Rhizophora spp.* soy protein phantom, was discussed in chapter five. In this chapter, the *Rhizophora spp.* soy protein phantom was simulated at high energy photon and electron beams using the established PRIMUS LINAC model. The physical phantom was also irradiated using the actual LINAC, while the dose was measured using the Gafchromic EBT2 film for comparison. The dose distributions from the MC calculations and the measurements were also validated by comparing them with the commercial solid water phantom. Finally, chapter six highlights the conclusion of this study, and the recommendations to improve this study for the near future.

CHAPTER 2

THEORY AND LITERATURE REVIEW

2.1 Radiation Beam Therapy

Radiation can be delivered in two ways, i.e. either externally or internally. External radiation therapy is the application of radiation that is produced by external sources. This treatment applies either photon or electron beam that is bombarded by a modality, e.g. the linear accelerator (LINAC) and Cobalt-60 machine. Figure 2.1 shows the LINAC, which is the common modality used in the radiotherapy department. In contrast, internal radiation therapy (in radiotherapy department) is being delivered via a brachytherapy machine, where the radiation sources are being located close to the tumour.

Figure 2.1: The linear accelerator (LINAC) that is commonly used in the radiotherapy department.

In general, the photon beam is being used to treat tumours located deep inside the patient’s body, whereas the electron beam is used to treat tumours that are more superficial, e.g. skin cancer. This is because, photon is a highly penetrative radiation and thus, are able to penetrate deeper into a material compared to the electron, which is a highly interactive (and thus, less penetrative) radiation. This penetrating ability depends largely on the beam energy.

The energy ranges commonly used for treatment with the photon beam is 6 to 18 MV, while for the electron beam is 6 to 20 MeV, since the photon and electron beams have different characteristics. Even though the photon beam can reach the deeper area, the electron beam offers more distinct advantages in terms of the radiation uniformity towards the target, and minimising the dose to the deeper tissues (Khan, 2010).

2.2 Monte Carlo Method in Radiotherapy Treatment Planning

Treatment planning system (TPS) is being used to estimate the dose distribution in a patient, as a result of a radiation treatment. The objective of the TPS is to ensure that the tumour receive the maximum dose possible, with uniform dose distribution. Rationally, it is impossible to treat a tumour without giving any radiation exposure to the surrounding tissues. However, the doses to the healthy tissues and critical organs can still be minimised, by optimising the irradiation parameters during the treatment planning procedure (Strydom, Parker, & Olivares, 2005.).

Pencil-beam, pencil-beam redefinition, collapse cone convolution, superposition/convolution and MC are various algorithms used by the TPS, to calculate the dose distributions (Aziz et al., 2011). International Commission on Radiation Units and Measurements (ICRU) recommends that the TPS should results in an accuracy of within 2 % or 2 mm. However, most of the current algorithms used in the clinical practice failed to fulfil this recommendation, where the deviations can go up to 5 % (AAPM TG-53; Caccia et al., 2007).

MC is defined as the numerical method with the ability to perform evaluations or calculate integrals based on the random number sampling (Fippel, 2013). The MC method was first introduced in the 1960s. Since then, it has been well-known and frequently used by the physicists, as it is one of the calculation methods that provides the best statistical solution. It has also be used as an option for problems that cannot be solved by a simple analytical approach (Mohammed et al., 2015; Reynaert et al., 2006b).

The main advantage of the MC method is its ability to compute doses on both the homogenous and inhomogeneous targets. The method was developed based on computational algorithms that solved problems by repeating the random sampling, in order to generate the results (Aziz et al., 2011). Apart from that, it has also been considered as an alternative to the analytical method, and serves as the ‘gold standard’ for the validation of radiation dosimetry measurements (Caccia et al., 2007; Abdel-Rahman et al., 2005).

The most interesting advantage of this method is the ability to precisely simulate photon and electron transports in a matter. It can also track individual particle in a radiation transport problem. This can be done by sampling the appropriate quantities from the probability distribution of the individual physical process. The quantities include particle fluence, energy spectrum and dose distribution, which can be calculated by simulating a large number of particle histories. On the other hand, the virtual experimental platform of various beam configurations provides a better understanding on the basic radiation physics.

The LINAC MC model needs to be built as close as possible to the actual LINAC, in order to precisely simulate the photon and electron beams. There are several factors that may affect the final model, such as the chosen MC dose engine, the provided details of information and the quality of the basic measurements (Júnior et al., 2015; Reynaert et al., 2007).

There are several MC dose engines that are currently available, i.e. Electron Gamma Shower (EGS), Geometry and Tracking (GEANT), Monte Carlo N-Particle (MCNP) and Penetration and Energy Loss of Positrons and Electrons (PENELOPE). These dose engines can be differentiated by their particle of interest and also the cross-section data.

The EGS and MCNP are the common dose engines used for clinical applications and are often utilised as benchmarks. The PENELOPE and EGS are more suitable to be use for simulating the photon and electron (positrons). Meanwhile, the MCNP and GEANT are suitable for studies involving photon beam with higher energies (18 MV and above) (Reynaert et al., 2007).

Since this study involved the application of photon (with energy of below 18 MV) and electron beams, thus the EGS was chosen. In addition, the process of modelling a LINAC using the EGS is much easier, due to its user friendly feature, with options for modification (Júnior et al., 2015). Thus, an accurate model can be established with a less complicated approach.

EGS was developed as part of a project between the National Research Council of Canada and the University of Wisconsin (Ahmed et al., 2014). It consists of two user codes that are specifically developed for the modelling of a LINAC and dose calculations.

The BEAMnrc/EGSnrc is a user code that was specifically developed for the modelling of a LINAC. This simulation phase requires information on the component module (CM) of the LINAC. Once completed, the information will then be compiled and the phase space data will be generated as the output. This output is important for use in the dose calculation. Meanwhile, the DOSXYZnrc/EGSnrc code is the program that calculates the dose based on the output obtained from the BEAMnrc/EGSnrc code. It allows the importing and translating of the CT data in voxel, and simulation of radiation interaction with a phantom.

Extensive reviews on the applications of MC method in medical radiation, especially in radiation therapy, have been carried out by previous researchers (Schreiber, Sawkey & Faddegon, 2012; Mihailescu & Borcia, 2014; Ahmed et al., 2014; Aljamal & Zakaria, 2013; Aubry et al., 2011; Kawrakow & Walters, 2006; Abdel-Rahman et al., 2005; Fix et al., 2004). This method has been much more appreciated because it can generate accurate results as expected in the measurements. Besides, the improvements of computer processors have contribute to a much realistic use of this method for clinical applications.

2.3 Accuracy of Monte Carlo Dose Calculation

The low accuracy of the current algorithm can introduce error and lead to wrong optimisation, which is called the convergence error (Reynaert et al., 2007). Other than its high accuracy, the MC method is also preferred as it can handle backscatter or scatter perturbation by air cavities, better than the other algorithms (Rogers et al., 1995).

Khan (2010) reported that the accuracy of dose calculation does not only depends on the LINAC model, input data and the limitation of the algorithm, but is also highly influenced by the grid spacing parameter, especially by the high dose gradient.

Besides, the number of the simulated particle history also affects the accuracy of the dose calculation. The particle history in dose calculation is related to the number of electron incidence on a phantom. A formula to estimate the number of particle history required for the simulation is shown in Equation 2.1.

$$N_\gamma = \frac{1}{\delta^2 \mu_{en}^{eff}} \frac{A_{beam}}{V_{voxel}}$$

(Eq 2.1)

where, μ_{en}^{eff}, A_{beam}, V_{voxel} and δ are the effective linear energy absorption coefficient for photons in water, the beam area, the volume of the dose scoring voxel and the statistical uncertainties of the dose (in the central part of the beam), respectively.

This formula is being applied when estimating the particle history in the treatment planning, for single or multiple beams. Increasing the particle history by the factor of 4 will reduce the uncertainties by a factor of 2 (Fippel, 2013).

As mentioned before, the accuracy of the dose calculation also depends on the model that has been established. The details and specific information are required to generate a good LINAC model. The dose calculations are sensitive to any changes in the LINAC. Tuning a CM on the treatment head may also affect the dose distribution. Verhaegen and Seuntjens (2003) summarised the factors that may affect the end results of the calculation, such as the primary electron energy beam, radial intensity distribution, opening of a primary collimator and information (material and density) of the flattening filter.

The LINAC model that has been established needs to be validated with the measurements obtained from the actual LINAC. Low uncertainty is expected to ensure that the model has been established and is accurate to be used for dose calculation. The most common way applied by the researchers to define the uncertainties is by comparison with the results from the measurements. The measurement includes measuring the dose using a dosimeter, such as film or ionisation chamber (IC).

There were also several other options recommended by Bouchard et al. (2013), to validate the LINAC model, such as by comparing the attenuation profile from the model with the manufacturer's data, and trace the photon ray that cross the boundaries between air and the last CM. However, these options were rarely used as it may result in a more complex task.

The accuracy of the Saturn43 LINAC model was successfully studied by Ahmed et al. (2014), where the EGSnrc dose engine was used for the dose calculation. The well agreement between the calculated and measured doses were observed in the dose distribution, at the percentage depth dose (PDD) curve and beam profile of the 12 MV photon beam.

The uncertainties of the build-up dose for high energy (6 and 18 MV) photon beam were studied by Abdel-Rahman et al. (2005). The data was obtained using the phantom-embedded extrapolation chamber (PEEC), which was made of solid water.

The validation of a LINAC model was performed by Aljamal and Zakaria (2013), where the dose calculation from two algorithms, i.e. MC and pencil-beam, were compared. Good agreement was observed between these algorithms, with percentage differences of 2 and 6 %, for PDD and beam profile, respectively. The result was sufficient to confirm that the model used in the study was accurate, for future dose calculations.

Another study by Jabbari and Hashemi (2009) was conducted to validate the accuracy of the NEPTUM 10PC LINAC, by comparing the dose calculation performed using the model with the measurement obtained using a diode detector. The model was successfully validated, where a perfect match was obtained between the dose calculation and the measurement.

The IC was used as a dosimeter by Aziz et al. (2011) to validate the dose calculation using 9 MeV electron beam produced by the Siemens PRIMUS LINAC. The result was then considered as a benchmark for their current study. Good agreement was successfully obtained between the dose distributions, with percentage difference of less than 2 %. Therefore, it was concluded that the model was accurate and ready to be used for dose calculation.

2.4 Efficiency of the Dose Calculation on MC Method

Apart from its superior performance, a large amount of computational resource and power are needed, in order the dose calculation using the MC method to be performed. Longer calculation time is required due to its complexity compared to the other algorithms. A larger amount of particles histories should be applied to achieve an accurate result, with the expense of an increase in the computational time. The efficiency of the MC dose calculation can be defined as in Equation 2.2.

$$\varepsilon = \frac{N}{Ns^2T} = \frac{1}{s^2T}$$

(Eq. 2.2)

where, N represents the number of simulated particle history, s^2 is the estimation of true variance for the quantity of the quality of interest, and T is the total central processing unit (CPU) calculation time required to reach the variance.

Since the accuracy of dose calculation is greatly influenced by the substantial number of particle history, techniques to reduce the calculation time while maintaining the accuracy were introduced. Variance reduction technique (VRT), such as range rejection, bremsstrahlung splitting and forced interaction, were suggested to reduce the computational time for the MC simulations (Rogers, Walters & Kawrakow, 2013a; Rogers et al., 1995).

Range rejection can save computing time by terminating the history. ECUTTER is a threshold energy that automatically rejects the particle with lesser energy and leaves the region without reaching the scoring plane. However, range rejection has a limitation where it does not work effectively for smaller voxels (2–3 mm) (Ma et al., 2002).

Bremsstrahlung splitting is created in the simulation process by combining several interactions, such as Compton scattering, pair production and photoelectric absorption, to achieve better efficiency. There are three types of bremsstrahlung splitting (BS), i.e. uniform BS (UBS), selective BS (SBS) and directional BS (DBS). Each of them contributes to the computing efficiency and is functionally dependent on the parameters of interest. However, the DBS is the most commonly used for simulation, as it offers the largest improvement in the efficiency (Jarkko, 2014).

Apart from the VRT, the efficiency of dose calculation can also be improved by increasing the voxel size. Reynaert et al. (2006b) reported that the voxel size has a direct effect on the calculation time. By increasing the volume of the phantom's voxel during the calculation will give a similar effect as doubling the particle history. However, excessively large voxel volume may lead to the averaging artefacts.

Kawrakow, Rogers and Walters (2004) compare the time taken for calculation with and without applying the DBS, for 6 MV photon beam. They found that the efficiency for the PDD curve was improved by a factor of 6.4, when the DBS was applied. The study was then continued for higher energy, i.e. 18 MV photon beam, and larger field size. It was found that, improvements by a factor of 3.5 and 7 were recorded by the DBS, for the energy and field size, respectively. Thus, it was concluded that the DBS was effective to reduce the calculation time.

A similar technique was conducted by Abdel-Rahman et al. (2005) and Kim, Hill and Kuncic (2012) to increase the efficiency of their simulation. They efficiency was successfully increased while at the same time maintaining an accurate result.

Meanwhile, the range rejection technique has been successfully performed in a previous study. Ma et al. (2002) considered applying the range rejection technique on their model. The effect of range rejection was investigated for different treatment sites, including the air, lung, soft tissue and bone. They found that the dose calculation was more efficient when applying the range rejection technique, by 10–30 times faster.

2.5 Beam Characteristics

The International Atomic Energy Agency (IAEA) TRS 398 (2000) listed the information required for clinical dosimetry, such as PDD and beam profile. The measurement is necessary for all the energies involved in radiotherapy. It is impossible to measure the PDD and beam profile on the patients, thus, it is performed using the water phantom or water equivalent material instead.

2.5.1 Percentage Depth Dose Curve

The measurement of the depth dose begins from the point on the phantom's surface, and down to its bottom. The PDD is the fraction of the dose at a certain point, normalised to the maximum dose on the central axis of the beam. It can also be defined as in Equation 2.3.

$$PDD = \frac{Dose\ at\ certain\ depth}{Dose\ at\ reference\ depth}\ x\ 100\ \%$$

(Eq. 2.3)

The typical PDD plotting at the central axis for photon and electron beams is illustrated in Figure 2.2. There are several important points and regions identified in the PDD curve, such as the surface dose, build-up region, depth of maximum dose (dmax) and exit dose.

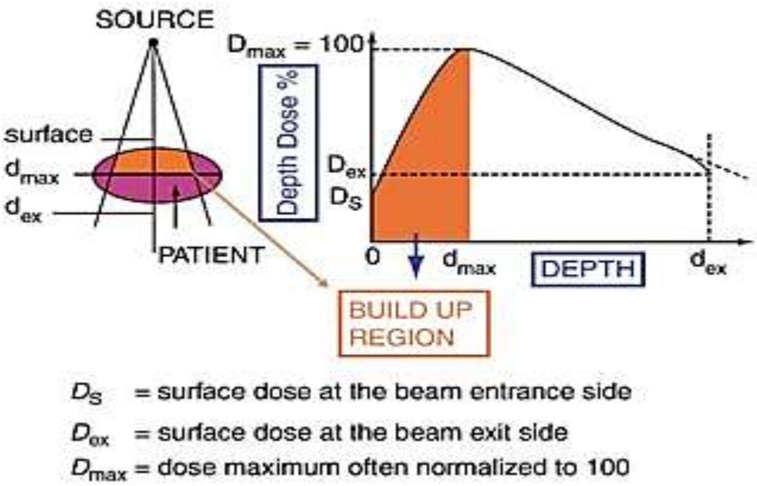

Figure 2.2: The typical depth dose curve

The surface dose should be lower than the maximum dose, and it relies on the beam energy and the estimated field size. Basically, the surface dose is contributed by the radiation scatter with the collimator or air, and backscatter from the phantom (Podgorsak, 2006). Low surface dose promotes the skin sparing effect, which has been an advantage for the photon beam.

The build-up region is the area located between the surface and the dmax. The build-up region for electron beam is much less pronounced than the photon beam, due to the impact of scatter interaction between the electrons and the absorber. The electrons are effortlessly scattered and result in a more rapid build-up, with a shorter separation.

The dmax depends on the beam energy and field size, and is usually set as the reference point to determine the depth dose for every energy. The exit dose refers to the dose at the exit point from the phantom. The exit dose differs for photon and electron beams. This is because the PDD curve for electron beam has a tail that is represented by the bremsstrahlung effect in the LINAC head, and also due to the interactions in the air between the exit window of the LINAC and the phantom.

In addition, the PDD curve for electron beam has specific dosimetric properties. There are several parameters that are used to describe the beam, such as the most probable energy on the phantom surface ($E_{p,0}$), the mean energy on the phantom surface ($\overline{E_0}$), and the depth at which the absorbed dose falls to 50 % of the maximum dose (R_{50}). The $E_{p,0}$ is related to the practical range $\left(R_p\right)$, as shown in Equation 2.4.

$$E_{p,0} = 0.22 + 1.09\,R_p + 0.0025R_p^2 \tag{Eq. 2.4}$$

where, $E_{p,0}$ is in megavoltage (MV) and R_p in cm. The $\overline{E_0}$ is related to the half value of R_{50}, as shown in Equation 2.5.

$$\overline{E_0} = CR_{50}$$

(Eq. 2.5)

where, C = 2.33 MeV/cm for water and R_{50} is in cm.

2.5.2 Beam Profile

The beam profile is measured at a specific depth in the phantom. It represents the dose at any point in a plane perpendicular to the beam direction, to the dose at the central axis of that plane. The beam profile comprises of three distinct fundamental regions, which are the centre, penumbra and umbra, as listed in Table 2.1 and illustrated in Figure 2.3.

Table 2.1: Regions of the beam profile

Regions	**Definition**
Central region	The central portion of the profile extends from the central axis of the beam, up to within 1–1.5 cm from the edge of the geometrical field.
Penumbral region	The dose rapidly changes and depends on the field defining collimator, the finite size of the focal spot and the lateral electronic disequilibrium.
Umbral region	The region outside the radiation field, far removed from the field edge.

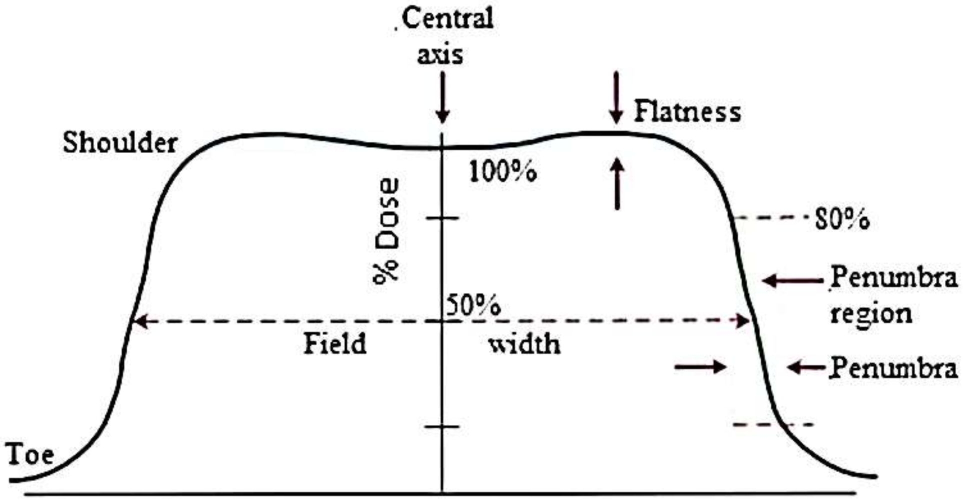

Figure 2.3: The typical beam profile (Gunderson & Tepper, 2012)

The uniformity along the centre of the beam profile determines the nature of the photon beam. It can be measured by two parameters, i.e. the beam flatness and symmetry. The recommended acceptance limits for the flatness and symmetry are less than 3 and 2 %, respectively (Strydom, Parker & Olivares, 2005.; Stanton & Stinson, 1996; AAPM Report 32.).

Zhang et al. (2009) explained that the beam symmetry can be determined from the maximum percentage deviation between the two opposite points on the beam profile (-x, x) from the central axis points, which is 80 % of the full width half maximum (FWHM). Meanwhile, the beam flatness can be calculated as in Equation 2.6.

$$F = \frac{D_{max} - D_{min}}{D_{max} + D_{min}} \, x \, 100 \, \%$$

(Eq. 2.6)

Where; *Dmax* and *Dmin* correspond to the maximum and minimum dose in the plateau area of the profile, respectively.

2.6 Basic Radiation Interaction with Matter

2.6.1 Photon Interaction with Matter

The MC method has been broadly utilised in the field of radiation therapy, since it can simulate the radiation interactions with matter. Photon interactions with matter by the MC method are based on four main principles, i.e. the photoelectric absorption, Compton scattering, coherent scattering and pair production.

Photoelectric absorption is predominant in high density material (high atomic number, Z). In this interaction, photons will interact with a tightly bound electron in the inner shell, as the energy of the photon is higher than the electron's binding energy. The photon transfers its energy to the electron, and the electron will be ejected, consequently leaving a vacant shell. Figure 2.4 illustrates the phenomenon of the photoelectric absorption. The ejected electron is known as a photoelectron. The kinetic energy of the photoelectron can be calculated using Equation 2.7

$$E_k = E_0 - E_b$$

(Eq. 2.7)

Where $E_k, E_0 \; and \; E_b$ are the kinetic energy of the photoelectron, energy of the initial input photon and the electron binding energy, respectively.